Published in final edited form as:
J Neuroendocrinol. 2009 February ; 21(2): 108–122. doi:10.1111/j.1365-2826.2008.01812.x.

FXYD1, a modulator of Na^+,K^+-ATPase activity, facilitates female sexual development by maintaining GnRH neuronal excitability

Cecilia Garcia-Rudaz[1], **Vivianne Deng**[1], **Valerie Matagne**[1], **Oline Ronnekleiv**[2], **Martha Bosch**[2], **Victor Han**[1], **Alan K. Percy**[3], and **Sergio R. Ojeda**[1]

[1]Division of Neuroscience, Oregon National Primate Research Center/Oregon Health & Science University, Beaverton, Oregon

[2]Department of Physiology and Pharmacology, Oregon Health & Science University, Portland, Oregon

[3]Department of Pediatrics University of Alabama at Birmingham, Birmingham, Alabama

Abstract

The excitatory tone to GnRH neurones is a critical component underlying the pubertal increase in GnRH secretion. However, the homeostatic mechanisms modulating the response of GnRH neurones to excitatory inputs remain poorly understood. A basic mechanism of neuronal homeostasis is the Na^+, K^+-ATPase-dependent restoration of Na^+ and K^+ transmembrane gradients after neuronal excitation. This activity is reduced in a mouse model of Rett syndrome (RTT), a neurodevelopmental disorder in which expression of FXYD1, a modulator of Na^+, K^+-ATPase activity, is increased. We now report that the initiation, but not the completion of puberty, is advanced in girls with RTT, and that in rodents FXYD1 may contribute to the neuroendocrine regulation of female puberty by modulating GnRH neuronal excitability. *Fxyd1* mRNA abundance reaches maximal levels in the female rat hypothalamus by the fourth postnatal week of life, i.e., around the time when the mode of GnRH secretion acquires an adult pattern of release. Although *Fxyd1* mRNA expression is low in the hypothalamus, about 50% of GnRH neurones contain *Fxyd1* transcripts. Whole-cell patch recording of GnRH-EGFP neurones revealed that the neurones of *Fxyd1*-null female mice respond to somatic current injections with a lower number of action potentials than wild-type cells. Both the age at vaginal opening and at first oestrous were delayed in *Fxyd1*$^{-/-}$ mice, but adult reproductive capacity was normal. These results suggest that FXYD1 contributes to facilitating the advent of puberty by maintaining GnRH neuronal excitability to incoming transsynaptic stimulatory inputs.

Keywords

Gene knockout; hypothalamus; GnRH neurones; female sexual development

Introduction

GABA and glutamate control GnRH secretion using a complex system of transsynaptic communication that involves both excitatory and inhibitory responses. Thus, GnRH neurones receive direct $GABA_A$ receptor-mediated excitatory inputs (1,2), and a $GABA_B$R-mediated inhibitory tone (3). They are also endowed with NMDA (4) and kainate (5)

Corresponding author: Sergio R. Ojeda, Division of Neuroscience, Oregon National Primate Research Center/ Oregon Health & Science University, 505 N.W. 185th Avenue, Beaverton, OR 97006. Tel.: (503) 690-5303; Fax: (503) 690-5384;E-mail: ojedas@ohsu.edu.

receptors that consistently stimulate GnRH release. The excitatory glutamatergic input to GnRH neurones (6,7) increases during development (5), reaching its highest level around the time of puberty (8). In addition to these direct inputs, amino acid neurotransmitters control GnRH secretion via mechanisms involving neuronal systems functionally coupled to GnRH neurones. Among these systems, GABA interneurones are thought to exert a major inhibitory control on GnRH secretion via presynaptic inhibition of neuronal systems (glutamate, norepinephrine, NPY) able to stimulate GnRH secretion (reviewed in (9)). In turn, hypothalamic GABA neurones receive a strong glutamatergic input (10), which would be expected to inhibit GABA release (11,12). It is thus obvious that specific mechanisms must exist to ensure the homeostatic modulation of such complex transsynaptic communication pathways controlling GnRH secretion.

Using GeneChip DNA arrays to study the brain of human subjects suffering from a neurodevelopmental disorder known as Rett syndrome (RTT), we observed that the expression of *FXYD1* (phospholeman), a gene that encodes a protein involved in the homeostatic regulation of cell function (13), is increased in the frontal cortex of these patients (14). RTT (OMIM #312750) is an X-linked neurodevelopmental disorder that ranks as the second most prevalent cause of mental retardation in girls (15). Most cases of RTT are associated with mutations of the gene encoding methyl-CpG-binding protein 2 (MeCP2) (16-18), which represses gene transcription by binding to 5-methylcytosine residues in symmetrically positioned CpG dinucleotides. Consistent with the notion that RTT is primarily due to a loss of MeCP2 function, *Mecp2*-null mice exhibit neurological abnormalities remarkably similar to those of RTT (19-21).

As seen in humans, *Fxyd1* expression is also increased in the cerebral cortex of these mutant mice (14). FXYD1 belongs to a family of small (30-130 amino acid) single-pass transmembrane proteins that have their C-terminus on the cytoplasmic side (13,22). The FXYD family was given this name because its members contain an invariable short PFXYD motif (proline-phenylalanine-X-tyrosine-aspartate) at the beginning of a 35 amino acid signature motif encompassing the transmembrane domain and adjacent regions (13). A major function of FXYD proteins is to regulate Na^+, K^+-ATPase activity in a tissue-specific manner (22). FXYD1 is highly expressed in heart and muscle, where it associates with α and β subunits of Na^+, K^+-ATPase, and decreases the affinity of Na^+ for the enzyme (23). In keeping with these findings, overexpression of FXYD1 in cardiac myocytes inhibits Na^+, K^+-ATPase activity and increases cell excitability (24). Should a similar mechanism operate in the brain, the inhibition of neuronal Na^+, K^+-ATPase activity by increased FXYD1 levels would be expected to reduce the ability of these cells to restore Na^+ and K^+ transmembrane gradients after neuronal excitation, causing hyperexcitability (25). Lowering the availability of FXYD1 would result in the opposite effect, i.e., hipoexcitability. FXYD7, another member of the family that is exclusively expressed in brain, also modulates Na^+, K^+-ATPase activity, but it does so by decreasing the K^+ affinity of the Na^+/K^+-ATPase pump (26).

The presence of FYXD1 and FXYD7 in the basal forebrain (14,26) raises the possibility that these proteins might be component of the homeostatic system that modulates the excitatory transsynaptic control of neuroendocrine neurones, including the GnRH neuronal network. The increased *FXYD1* expression observed in RTT also raises the question as to the normalcy of the pubertal process in girls affected by RTT. We now show that the onset of puberty, as assessed by the initiation of breast development, is accelerated in a large cohort of ethnically homogeneous girls with RTT. We also observed that both the *Fxyd1* and *Fxyd7* genes are expressed in the developing female rat and mouse hypothalamus, that at least 50% of GnRH neurones contain *Fxyd1* mRNA, and that the absence of *Fxyd1* results in decreased GnRH neuronal excitability. In accord with the advancement of puberty seen in RTT patients, acquisition of female reproductive capacity was delayed in *Fxyd1*$^{-/-}$ mice. As in

RTT patients, this alteration in the timing of puberty was transient, suggesting the activation of compensatory mechanisms.

Material and Methods

Human subjects

Clinical data on Tanner stages and the onset of menstruation were gathered as part of the Rare Disease Clinical Research Centre (RDCRC) Rett syndrome (RTT) study funded by the NIH through the Office of Rare Diseases (ORD) and the National Centre for Research Resources (NCRR). Participants were evaluated twice yearly through age 12 and annually thereafter. Tanner staging was assessed at each visit using established criteria and onset of menstruation was recorded. For this analysis, Tanner staging and menstruation onset data were available from 494 participants with classic RTT. More than 90% had a pathogenic mutation in *MECP2*. The RDCRC RTT study has been approved by the IRBs at the respective consortium sites: Baylor College of Medicine, Greenwood Genetic Centre, and University of Alabama at Birmingham. All data were acquired following informed consent through the Rare Disease CRC approved protocol at the respective sites.

Animals

Because the neuroendocrine and phenotypic changes associated with the onset of female puberty have been extensively studied in rats and, therefore, are much better characterised than in mice (for a review see (27)), we used rats to examine the changes in *Fxyd1* and *Fxyd7* mRNA expression that occur in the hypothalamus during sexual maturation, and to define by *in situ* hybridisation the cellular sites of these two genes in the brain of immature animals. We used mice to define the effect of deleting the *Fxyd1* gene on female reproductive development and on the electrophysiological properties of GnRH neurones.

Sprague Dawley rats (Harlan, Indianapolis, IN) arrived at the laboratory when they were either pregnant or 21-days of age. They were housed under controlled conditions of temperature (23–25 °C) and light (14 h light, 10 h dark; lights on from 0500–1900 h). Food (Purina laboratory chow, Ralston-Purina, St. Louis, MO) and water were provided *ad libitum*. *Fxyd1*$^{-/-}$l mice (28) were maintained on a C57/BL/6 background. For electrophysiology studies, *Fxyd1*$^{-/-}$ males were bred to transgenic females mice expressing enhanced green fluorescent protein (EGFP) under the control of the GnRH promoter (EGFP-GnRH) (29), and also maintained on a C57/BL/6 background. To assess the effect of a *Fxyd1* deficiency on female puberty and reproductive function, *Fxyd1* heterozygotes were crossbred to generate wild-type and *Fxyd1*$^{-/-}$ mice in the same litter. The mice were housed under controlled temperature and photoperiod (light on at 0600 h and off at 1800 h) and given free access to food and water. Animal usage was duly approved by the Institutional Animal Care and Use Committee of the Oregon National Primate Research Centre.

Phases of puberty

To determine the changes in hypothalamic *Fxyd1* and *Fxyd7* mRNA abundance during prepubertal and peripubertal development of female rats, groups of animals were euthanised at different times of postnatal (PN) life (neonatal period: PN day 0 and 6; infantile period: PN days 12 and 18, juvenile period: PN days 24 and 30), and during the time of puberty (days 30 to 36). In this case, the rats were killed first and then classified in different phases of puberty, according to criteria previously established (27). According to these criteria, 30-32 day-old rats are considered to be in the late juvenile (LJ) phase. At this time, the vagina is not yet patent and the uterine weight is 60 mg or less, with no accumulation of intrauterine fluid. Animals with enlarged uteri and detectable intrauterine fluid are considered to be initiating puberty; as such, they are classified to be the early pro-oestrous

(EP) phase of the pubertal process. Animals showing a uterus ballooned with fluid and a uterine weight of at least 200 mg are in late pro-oestrous (LP), the phase of puberty when the first preovulatory surge of GnRH and gonadotrophins takes place. The first ovulation occurs the following day, on the first oestrous (E). At this time, the vagina becomes patent exhibiting a cytology of cornified cells, and fresh corpora lutea can be readily visualised in the ovaries. We used the presence of corpora lutea to confirm the time at first ovulation.

Genotyping

To identify *Fxyd1* genotypes we used three sets of primers, employed together in a single PCR reaction. The primers FXYD5-a (5′-CTTAAGTCCTTAGGCCGTCC-3′), Fxyd5-B (5 ′-GATCATCGCGAGCCATGC-3 ′) and FXYD5-c (5 ′- CCGTAGGTGAATGGATCC-5′) amplify a band of 584 bp from the wild-type (WT) allele and a 213 bp band from the deleted (KO) allele (28).

Real- time PCR

The mRNAs encoding rat (r)*Fxyd1* (NM_031648) and r*Fxyd7* (NM_022008v1) were measured in the medial basal hypothalamus (MBH) and frontal cortex (FC) of developing female rats by real-time PCR, as previously described (30,31) After reverse transcribing 200 ng of total RNA, aliquots of each reaction (10 ng cDNA/μl) were diluted 1:10 before using 2 μl for real-time PCR. Each sample was run in triplicate along with a relative and an absolute standard curve. Relative standard curves, generated by serially diluting one sample 1:10 to 1:10,000 times, served to estimate the content of 18S ribosomal RNA of each sample. The primers used to detect 18s ribosomal RNA were purchased as a kit (TaqMan Ribosomal RNA Control Reagents Kit, Perkin Elmer Applied Biosystems, Foster City, CA). Absolute standard curves were constructed by using serial dilutions (1:10) of sense RNA (2 ag-2 ng). The threshold cycle number (C_T) from each sample was referred to this curve to estimate the corresponding RNA content, and each RNA value was then normalised for procedural losses using the 18S ribosomal RNA values estimated from the relative standard curve. C_T was the fractional cycle number at which the fluorescence accumulated to a level 10 times greater than 1 SD from basal values. The primers and the fluorescent probe for real-time PCR were selected with the assistance of the programme, Primer Express (Perkin Elmer Applied Biosystems). The primer sequences (Invitrogen Life Technologies, Carlsbad, CA) for *rFxyd1* were: forward (5′-AGCTCCGCAGGAACCAGAT-3′) and reverse (5′-TGATAAGGATGCCCAAGATGAA-3′). For *rFxyd7*, they were: forward (5′ TATGCCACCGTGCAGACTGT-3′) and reverse (5′-TCCGCCTTCCTGCACTTAA-3′). The internal fluorescent oligodeoxynucleotide probe (Perkin Elmer Applied Biosystems) sequence was 5′-ACGATTACCACACCCTGCGGATCG-3′ for *rFxyd1* and 5 ′-CCCAGCACGAACATGATAGTGGCCA-3′ for *rFxyd7*, respectively. Real-time PCR reactions were performed in a total volume of 10 μl, each reaction containing 2 μl of the diluted reverse transcribed sample or 2 μl of standard, 5 μl TaqMan Universal PCR Master Mix (PE Applied Biosystems), 250 nM of each gene specific- and ribosomal fluorescent probes, 300 nM of each gene specific primer, and 10 nM of each ribosomal primer. The real-time PCR programme used consisted of an initial annealing period of 2 min at 50 °C, followed by 10 min of denaturing at 95 °C, and 40 cycles of 15 sec at 95 °C and 1 min at 60 °C.

Semi-quantitative PCR

The loss of *Fxyd1* mRNA in the brain of *Fxyd1*$^{-/-}$ mice was confirmed by semi-quantitative PCR using total RNA from the MBH. The PCR was carried out using Hotstart Taq polymerase (Qiagen, Valencia, CA) and 1 μl of cDNA as the template. The cDNA encoding cyclophilin, a housekeeping gene, was amplified in separate tubes, but using the same PCR conditions. The PCR conditions employed were: 5 min at 95 °C, 30 sec at 94 °C, 30 sec at

60 °C, and 1 min at 72 °C, repeating step 2 to 4 for 34 times, with a final extension of 10 min at 72 °C. The Fxyd1 primer sequences employed were: 5′-CAACAGGGGACAGCGTGAAT-3′ (forward) and 5′-TGGAGTCAGGTGGAGGTTCTA-3′ (reverse). The resulting PCR product had a length of 323 bp. The cyclophilin primer sequences employed were: 5′-GGCAAATGCTGGACCAAACACAA-3′ (forward), and 5′-GGTAAAATGCCCGCAAGTCAAAAG-3′ (reverse). This PCR reaction yielded a product of 223 bp. Each PCR reaction contained 25 pmol of each Fxyd1 primer and 10 pmol of each cyclophilin primer.

In situ hybridisation

The brains of immature female rats and mice (28 to 30 days of age) were fixed by intracardiac perfusion of 4% paraformaldehyde-borate buffer, pH 9.5. Both solutions were made with 0.1% diethyl pyrocarbonate (DEPC)-treated water to minimise RNase contamination. After dissection of the brain, tissue blocks were post-fixed overnight in the same fixative containing 20% sucrose, then blocked and frozen on dry ice, and stored at -80 °C until sectioning (32,33). The sections (30 μm) were cut on a sliding microtome, mounted on Superfrost Plus slides (Fisher Scientific, Santa Clara, CA), dehydrated under vacuum overnight and then frozen at -80 °C until processing for hybridisation. The hybridisation procedure was that recommended by Simmons *et al.* (34), as described earlier by us (33,35), using ^{35}S-UTP-labelled *Fxyd1* or *Fxyd7* cRNA probes (see below). Control sections were incubated with sense probes transcribed from the same plasmids, but linearised on the 3′ end to transcribe the coding strand of the cDNA template. Following an overnight hybridisation at 55-56 °C, the slides were washed and processed for cRNA detection (34). After dehydration, the slides were dipped in NTB-2 emulsion (Roche Diagnostics, Indiana, IN), and were exposed to the emulsion for three weeks at 4 °C. At this time the slides were developed, stained with 1% thionein, quickly dehydrated, dried, and cover-slipped for microscopic examination.

The *Fxyd1* cRNA probe used was transcribed from a 327 bp cDNA fragment amplified by PCR from the mouse cerebral cortex and cloned into the plasmid pGEM-T. This fragment contains the sequence comprised between nucleotides 83 and 406 in mouse *Fxyd1* mRNA (NM_019503). The *Fxyd7* cRNA probe was transcribed from a 310 bp cDNA amplified from rat cerebral cortex and also cloned into pGEM-T. This cDNA contains a sequence comprised between nucleotides 52 and 361 in rat *Fxyd7* mRNA (NM_022008).

Single cell PCR (scPCR)

Five intact transgenic (35-40-day-old) peripubertal female mice expressing EGFP under the control of the GnRH promoter (EGFP-GnRH) were used for scRT-PCR experiments. For cell harvesting, the animals were anaesthetised with ketamine/xylazine (1 mg and 0.1 mg/10 g, respectively) and killed by decapitation. The brain was rapidly removed from the skull and a block containing the diagonal band-preoptic area (DB-POA) was immediately dissected. DB-POA slices (300 μm) were cut on a vibratome and placed in an auxiliary chamber containing oxygenated artificial cerebrospinal fluid (aCSF). The slices are allowed to recover for 1–2 h in the chamber before dispersion. A discrete region of the DB-rostral POA was microdissected and incubated in 10 ml aCSF (124 mM NaCl, 5 mM KCl, 2.6 mM NaH_2PO_4, 2 mM $MgSO_4$, 2 mM $CaCl_2$, 26 mM NaHCO3, 10 mM Hepes, 10 mM D-glucose, in RNase-free water (Pyrogard-D filtered water, Millipore, Billerica, MA, USA), pH 7.3, 300 mOsm) containing 1 mg/ml protease for 17 min at 37 °C. The tissue was then washed four times in low calcium CSF (0.1 mM $CaCl_2$) and two times in aCSF. The cells were isolated by trituration with flame-polished Pasteur pipettes. The cells were dispersed onto a 60-mm glass bottom Petri dish, and were visualised under a Leica inverted

microscope equipped with fluorescence illumination (Leica Microsystems, Wetzlar, Germany). The fluorescence cells were patched and then harvested into the patch pipette by applying negative pressure. Samples of aCSF in the vicinity of the cells were also harvested. The contents of the pipette were expelled into a siliconised microcentrifuge tube containing 1 μl 5X colourless GoTaq Flexi buffer (Promega), 15 U RNasin, 0.5 μl 100 mM DTT and diethylpyrocarbonate (DEPC)-treated water in a 5 μl volume. The harvested cell solution and 25 ng of hypothalamic total RNA were denatured for 5 min at 65 °C, then cooled on ice for 5 min. Single-stranded cDNA was synthesised from cellular mRNA in a reaction containing 50 U MuLV reverse transcriptase, 3 μl 5X colourless GoTaq Flexi buffer, 5 mM $MgCl_2$, 0.625 mM dNTPs, 15 U RNasin, 10 mM DTT and 100 ng random hexamers in a total of 15 μl DEPC-treated water (Ambion, Austin, TX, USA) for a final volume of 20 μl. Cells and tissue RNA used as negative controls were processed as described above but without reverse transcriptase. The reaction mixtures were incubated at 42 °C for 60 min, denatured at 99 °C for 5 min and cooled on ice for 5 min.

The PCR reactions were performed using 3 μl of cDNA template from each RT reaction in a 30 μl PCR volume containing: 6 μl 5X colourless GoTaq Flexi buffer, 2 mM $MgCl_2$, 0.33 mM dNTPs, 2 U Taq DNA polymerase (Promega), 0.22 μg TaqStart Antibody (Clontech, Oxford, UK) and 50 pmol each of forward and reverse oligonucleotides. The mouse (m)Fxyd1 forward primer employed had a sequence (5′-CCGGATCCATTCACCTACGAT-3′) corresponding to nucleotides 245-264 in m*Fxyd1* mRNA (NM_019503). The reverse primer sequence (5′-GCAGTCAGGTGGAGGTTCTA-3′) is complementary to nt 446-465. The resulting PCR product was 220 bp in length. The mFxyd7 forward primer (5′-GCCTCAGCATTCAGCAACC-3′) corresponds to nucleotides 33-51 in mFxyd7 mRNA (NM_022007) and the reverse primer (5′ CAGGGACAGCAGTGGAAATCT-3” is complementary to nucleotides 322-342. The resulting PCR product is 309 bp in length. To confirm that the harvested fluorescent cells were indeed GnRH neurones, we PCR-amplified a 239 bp GnRH cDNA from each cell, using a forward primer corresponding to nt 21-40 in GnRH mRNA (NM_008145) and an antisense primer complementary to nt 240-259.

Taq DNA polymerase and TaqStart Antibody were combined and incubated at room temperature for 5 min. Then, the remainders of the reaction contents were added to the tube. Fifty cycles of amplification were performed using an MJ Research Dyad PTC-220 thermocycler (MJ Research, Inc., Waltham, Massachusetts, USA, [currently BioRad, Hercules, CA]) in 0.5 ml thin walled PCR tubes according to the following protocol: 5 min at 95 °C; 50 cycles of 30 s at 94 °C; 30 s at 60 °C; and 1 min at 72 °C, with a final 5 min extension at 72 °C. Ten μl of the PCR products were visualised with ethidium bromide on a 1.5% agarose gel. The scRT-PCR products for GnRH, *Fxyd1* and *Fxyd7* were confirmed by sequencing. In addition to the controls described above, aCSF harvested in the vicinity of the dispersed cells and water blanks were used as a control in the RT-PCR reaction.

Electrophysiology

A total of eight 28-30-day-old female mice were used for electrophysiological observations. All results were recorded using the whole-cell patch-clamp method in acute slice preparations.

Slice Preparation—The animals were deeply anaesthetised with halothane and rapidly decapitated. The skull was opened and the brain was irrigated with ice-cold, aCSF. The brain was removed and transferred to ice-cold aCSF for 1 minute to harden. In preparing transverse slices of the POA, two vertical cuts were made in the transverse plane; one just rostral to the optic chiastic, and another just caudal to the anterior commissure. After

trimming off the cortical tissue, the caudal surface was glued to a microtome block. The brain blocks were supported during cutting by a U-shaped wall of gelatin (12.5% in 0.1 M PB, pH7.3-7.4) that was glued behind the brain blocks on the opposite side from the blade. The same gelatin gel (in liquid form at about 30 °C) was poured between the gelatin wall and the surface of the brain to provide further support. The cutting chamber was filled with ice-cold aCSF during slicing. The composition of aCSF was as follows (in mM): NaCl 124, KCl 2.0, KH_2PO_4 1.25, $NaHCO_3$ 24, $CaCl_2$ 2.6, $MgSO_4.7H_20$ 1.6, glucose 20. Osmolarity 295-305, pH 7.2-7.4 after bubbled with 95% O_2 and 5% CO_2.

Slices were cut on a vibratome (Leica VT1000) at 200 μm and immediately transferred to a warm bath where they were kept submerged at 32-34 °C. Up to this point, the cutting solution contained the low affinity AMPA type glutamate receptor antagonist kynurenic acid (1 mM) to reduce potential excitotoxic damage (36). The slices were kept in the warm bath for about 30-60 minutes and then maintained in aCSF without glutamate blocker at the same temperature until recording.

Recording and stimulation—A single slice cut rostral to the anterior commissure was selected and transferred to a submerged recording chamber that was continuously perfused with bubbled, warm, (32-34 °C) aCSF at a rate of 1.5-2.5 ml/min. GFP-labelled cells were selected for whole-cell patch-clamp recording.

The electrodes used for whole-cell patch recording had resistances of 4-8 MΩ after being filled with an internal solution. The composition of the internal solution was as follows (in mM): K gluconate 130, EGTA 5, HEPES 10, KCl 3, $MgCl_2$ 2, Na_2 ATP 4, Na_2 phosphoreatine 5 and Na_2 GTP 0.4 (pH ~7.4, osmolarity 280-290). The patch pipettes were advanced with a MP285 manual manipulator (Sutter Instruments). The fluorescent cells were first identified with epiflurorescence using fluorescein filters, and visualised under infrared Nomarski optics using the 40X water-immersion objective of an upright microscope (Axoscope I, Zeiss). A gigaohm seal was formed by applying negative pressure to the recording pipette, and the membrane was ruptured by further negative pressure or by a zap (a brief current pulse generated by the amplifier). The recordings were performed under both voltage and current clamp modes using the Multiclamp 700A amplifiers (Axon Instruments, Forster City, CA). The initial holding potential under voltage clamp was -70 mV unless otherwise noted (see below). P-clamp 9 software (Axon Instruments) was used for data acquisition and analysis. To examine the intrinsic firing properties, current pulses of 300-500 ms from -150 to 250 pA (25 pA increments) were injected into the soma under current clamp to evoke spikes while cell was held at a membrane potential of -60 mV. To measure the input resistances, a small voltage (5 mV) or current (10-25 pA) pulse was injected to the soma. To determine firing patterns, 10-100 pA positive current was usually injected into the soma under current clamp to depolarise the cell to threshold for spiking. To examine miniature excitatory postsynaptic currents (mEPSCs), signals were recorded at -70 mV in voltage-clamp mode in the presence of the sodium channel blocker tetrodotoxin (TTX, 1 μM) and the $GABA_A$ receptor antagonist picrotoxin (100 μM). The AMPA type glutamate receptor antagonists CNQX and/or the NMDA type glutamate receptor antagonist AP5 were bath-applied in some cases to ensure the specificity of these receptors for the mEPSCs. The whole-cell patch recordings were discontinued when leak current exceeded 100 pA under voltage clamp or when membrane potential fell below -50 mV under current clamp. All drugs and chemicals were purchased from Sigma.

Clampfit 9 (Axon Instruments), Mini Analysis Programme V603 (Synaptosoft Inc., Leonia, NJ) and Origin 7 (OriginLab) were used for data analysis. The Student's t test was performed to assess the statistical significance, and results were presented as mean ± SEM.

Assessment of female puberty and female reproductive competence

Fxyd1 heterozygote mice were setup in breeding cages containing one adult male and two females. The resulting WT and KO female pups were housed in groups of 4-5 per cage at 21 days of age. The mice were then observed daily for vaginal opening. The day of vaginal opening, the animals were caged individually with one adult WT male to determine the interval to the first fertile cycle and the interval between litters. The cages were then inspected daily for new litters. The number of litters produced and the number of pups born per litter were also recorded. The age at the first oestrous was calculated by subtracting the gestation length time (22 days in mice) to the chronological age at the first litter.

Statistics

Quantitative data was analysed using SigmaStat 3.1 software (Systat Software Inc., San Jose, CA). The data were first subjected to a normality test and an equal variance test. Data that passed these two tests were then analysed using the Student's *t* test when comparing two groups, and one way repeated measures ANOVA followed by Student-Newman-Keuls multiple test for individual means when comparing multiple time points.

Results

The initiation of puberty in girls with RTT

A total of 494, largely (> 91%) white, girls affected by RTT were prospectively analysed for signs of puberty, and found to have achieved a Tanner stage 2 of breast development at an average age of 7.1 ± 2.5 (SD) years. Although it may not entirely valid to compare statistically the results of two different studies, this figure is earlier than the average age at Tanner stage 2 (9.96 ± 1.8 years of age; $p<0.01$) previously reported for a large (>15,000) cohort of normal white girls (37). Despite this earlier activation of the pubertal process, the age at first menstruation (12.7 ± 2.4) was similar to that reported for normal girls (12.9 ± 1.2), indicating that the completion of puberty is not accelerated, perhaps due to the activation of compensatory mechanisms. Interestingly, girls with RTT had an earlier initiation of breast development despite of being small for age in terms of weight and height/length, and having body mass indices correspondingly below those of normal females (not shown). Even more intriguingly, RTT patients failed to show the pubertal growth spurt in weight and height seen in normally developing controls, suggesting that this fundamental somatic change of puberty fails to occur in RTT.

Developmental expression of *Fxyd1* and *Fxyd7* mRNAs in the female rat hypothalamus

Fxyd1 mRNA abundance was low in the MBH of female rats at the time of birth and increased during neonatal-infantile development (PN day 6-18), to reach maximal values during the mid-to-late juvenile period (PN day 24-30). The increase was more pronounced during the transition between the infantile and juvenile development (PN days 18-24), i.e. at the time when GnRH release acquires a mature pattern of pulsatile release (38,39). At the time of puberty (PN day 30-36), *Fxyd1* mRNA content was measured in both the MBH without the median eminence (ME) and in the isolated ME. Although *Fxyd1* mRNA expression tended to decrease between LJ and LP in the MBH without the ME (MBH-), the only significant change ($p<0.05$) was an increase that occurred on the day of the first dioestrous (D1), i.e. after the first ovulation had taken place (Fig. 1B). In the ME, *Fyxd1* mRNA prevalence increased slightly between LJ and E, and then significantly ($p<0.01$) at D1 (Fig. 1C), broadly mimicking the changes in *Fxyd1* mRNA content seen in the MBH(-). In the FC, Fyxd1 mRNA abundance increased linearly between PN day 0 and the day of D1 (Fig. 1D).

In contrast to these patterns of expression, Fxyd7 mRNA abundance in the MBH was most elevated during neonatal days and the first half of the infantile period (PN days 0-12), decreasing at the end of this phase (PN day 18; $p<0.05$ vs. PN day12), to remain constant throughout juvenile development (PN days 24-30) (Fig. 2A). *Fyxd7* mRNA expression did not change significantly during puberty in either the MBH- (Fig. 2B) or the ME (Fig. 2C). In marked contrast to the decrease in *Fxyd7* expression seen in the MBH between birth and puberty, *Fxyd7* mRNA abundance in the FC increased linearly between the day of birth and the D1 phase of puberty (Fig. 2D).

Cellular localisation of Fxyd1 mRNA in the rat and mouse brain

A general *in situ* hybridisation view of the sites where the *Fxyd1* and *Fxyd7* genes are expressed in the brain revealed that *Fxyd1* mRNA is particularly abundant in ependymal cells (EC) lining the lateral ventricles of the brain (Fig. 3A) and also the latero-ventral lining of the third ventricle (Fig. 3B). Positive ependymal cells in this latter region include those located at the level of the organum vasculosum of the lamina terminalis (OVLT) (Fig. 3A, arrows), and tanycytes (T) lining the ventral aspect of the ventricle at the level of the MBH (Fig. 3B, arrows). Another tissue extremely rich in *Fxyd1* mRNA transcripts is the choroid plexus (CP) (Fig. 3B, arrows). In agreement with earlier studies (14,40), *Fxyd1* expression was low throughout the brain, including the FC and the hypothalamus (Fig. 3 A and B). In contrast to this distribution pattern, *Fxyd7* mRNA was especially abundant in the cerebral cortex (Fig. 3C, arrows), and ventromedial nucleus (VMH) of the hypothalamus (Fig. 3D, arrows), but was absent from the CP and cells lining the cerebral ventricles (Fig. 3C, D).

A more detailed examination of the POA (where GnRH neurones are located), showed the presence of *Fxyd1* mRNA transcripts in cells scattered throughout this region, but more predominantly in cells associated with the OVLT (Fig. 3E). In the MBH, the *Fxyd1* gene was most abundantly expressed in tanycytes of the third ventricle (Fig. 3F, arrows; higher magnification shown in panel K). As a comparison, Fig. 3G depicts a view of the CP, whose cells have a remarkable abundance of *Fxyd1* mRNA transcripts. As previously shown by our group (14), no hybridisation was detected in sections incubated with the sense *Fxyd1* RNA probe (not shown).

Higher magnification images of *Fxyd7* mRNA containing regions verified the abundance of *Fxyd7* mRNA transcripts in cells of the CTX (Fig. 3H), the paucity of expression at the level of the POA (Fig. 3I), and the high prevalence of these transcripts in the VMH (Fig. 3J and L, arrows). Most of the hybridisation signal in this region, as well as in the CTX was observed on cells that appear to be neurones because of their large, pale nuclei (Fig. 3L, examples denoted by arrows). Like in the case of *Fxyd1*, sections incubated with a sense *Fxyd7* RNA probe showed no specific hybridisation (not shown).

Expression of *Fxyd1* mRNA in GnRH neurones

To precisely determine if the *Fxyd1* gene is expressed in GnRH neurones, we measured *Fxyd1* mRNA levels in these cells using the technique of single cell PCR. Thirty-five EGFP-GnRH neurones from five intact peripubertal (35-40-day-old) female mice (a mean of 7 cells per animal) were harvested and confirmed by RT-PCR to express GnRH. These neurones were further analysed to determine *Fxyd1* and *Fxyd7* mRNA expression. As shown in Fig. 4, all of the neurones expressed GnRH. In addition, both the *Fxyd1* and *Fxyd7* genes were expressed in sub populations of GnRH neurones. Fifty-three ± 15.9% of GnRH neurones expressed *Fxyd1* mRNA transcripts, whereas *Fxyd7* mRNA was detected in 23 ± 8% of GnRH neurones. Both transcripts were expressed in 15 ± 10% of the cells.

The absence of FXYD1 decreases GnRH neurone excitability

To determine if FXYD1 plays a role in regulating GnRH neuronal activity, we crossed *Fxyd1*$^{-/-}$ males with GnRH-EGFP transgenic females, and generated F2 mice that were *Fxyd1*$^{-/-}$/GnRH-EGFP positive. RT-PCR assessment of *Fxyd1* mRNA abundance in the hypothalamus of these animals verified the absence of *Fxyd1* expression (Fig. 5A). Next, we used 28-day-old female mice for electrophysiological recording of GnRH-EGFP neurones. All neurones recorded were located in the medial (m) POA. Within this region, some were located near the third ventricle (central mPOA), and others were positioned more dorsally and laterally (dorso-lateral mPOA). Both groups of cells are similar in their somatic size and shape and in their dendritic pattern, but cells in the dorso-lateral mPOA appear to have longer dendritic arbors compared to cells in the central mPOA. A total of 51 WT and 46 *Fxyd1*$^{-/-}$ cells were recorded; of them, 19 WT cells and 28 *Fxyd1*$^{-/-}$ cells were in the central mPOA; 32 WT cells and 18 *Fxyd1*$^{-/-}$ cells were in the dorso-lateral mPOA.

Within both the WT and *Fxyd1*$^{-/-}$ groups, GnRH neurones located in central and dorso-lateral regions of the POA had similar resting membrane potentials. Likewise, resting membrane potentials were not different between WT and KO neurones (-69.7 ± 2.00 mV [range from -58 to -72 mV, n=15] in the WT group, and -65.4 ± 1.68 mV [range from -52 to -77 mV, n=19] in the *Fxyd1*$^{-/-}$ group ($p>0.05$). These values, though higher than in other brain neurones, are comparable to those previously reported for GnRH neurones, using the same GnRH-EGFP transgenic mice (29). In contrast to the lack of changes in resting membrane potential, the mean input resistance measured in *Fxyd1*-deficient GnRH neurones located in both the central and dorso-lateral mPOA was lower ($p<0.05$) than in WT neurones (Table 1). Interestingly, for both genotypes, the input resistance was significantly lower ($p<0.05$) in cells present in the dorso-lateral mPOA than in the central mPOA (Table 1).

The vast majority of the GnRH cells we examined were silent under resting conditions. Although three GnRH neurones (two Wt, one in the central mPOA and one in the dorso-lateral mPOA, and one *Fxyd1*$^{-/-}$ in the central mPOA) fired action potentials spontaneously, positive current steps of 10-200 pA were required in all other cells to depolarise them to approximately -45 mV and fire action potentials, which disappeared when the slices were exposed to the Na^+ channel blocker TTX (1 μM). Despite this similarity at resting conditions, responses of these cells to somatic current injections were different between *Fxyd1*$^{-/-}$ and WT animals. Examples of such recordings are shown in Fig. 5. Panels B and C show the response to depolarisation current steps of 300 ms (15 pA increments) of GnRH cells from *Fxyd1*$^{-/-}$ mice animals located in the central mPOA (B) and dorso-lateral mPOA (C). Regardless of the cell location, the depolarisation current steps elicited a low number of action potentials (2 and 5, respectively). GnRH neurones from WT animals, located in the same areas, responded to the same current steps with 21 and 24 action potentials, respectively (Fig. 5 D, E). Quantitative analysis of the results indicated that the spike numbers shown by GnRH neurones in the central or dorso-lateral mPOA were not different among *Fxyd1*$^{-/-}$ mice or among WT animals, but that the number of elicited action potentials shown by *Fxyd1*$^{-/-}$ GnRH neurones was significantly ($p<0.01$) lower than the number of action potentials exhibited by cells from WT animals, (Fig. 5F; 3.2+/- 2.47; n=10 cells vs. 22+/-3.76 spikes, n =12 cells, respectively).

All GnRH neurones in the central mPOA showed pronounced fast after-hyperpolarisation (fAHP), regardless of the presence or absence of *Fxyd1* (Fig. 5B and D). However, only about half of cells in the dorso-lateral mPOA had such a response. The mean amplitude of fAHP in *Fxyd1*$^{-/-}$ cells located in both the central and dorso-lateral mPOA was significantly ($p<0.05$) greater than that of WT cells (Table 1). Examples of these responses are depicted to the right of panels B, C (cell in the central mPOA) and D, E (cell in the dorso-lateral mPOA).

Miniature excitatory postsynaptic currents (mEPSC) were also examined in voltage clamp mode after blocking voltage-dependent Na^+ channels and $GABA_A$ receptors with the antagonists TTX and bicuculline, respectively. The mEPSCs ranged from 10-50 pA in amplitude and from no events to a few events per minute. The mEPSCs were not affected by bath application of the NMDA type of glutamate receptor antagonist AP5, but disappeared by adding the AMPA type glutamate receptor antagonist CNQX to the bath (not shown). Examples of such recordings are shown in Figure 6. Panels A and B show cells recorded from *Fxyd1*$^{-/-}$ animals located in the central (A) and dorso-lateral (B) mPOA. Panels C and D show cells recorded from WT animals. In general, cells in the central mPOA were much less active than those in the dorso-lateral mPOA, with a predominance of cells in the central POA being silent in both *Fxyd1*$^{-/-}$ and WT animals (24 silent cells vs. 4 active of 5 recorded cells in *Fxyd1*$^{-/-}$ mice, and 19 silent cells vs. 0 active of 3 recorded cells in WT animals). Active cells in the dorso-lateral mPOA had a mEPSC amplitude of 13.57 ± 0.80 in WT animals as compared with 13.25 ± 1.13 in *Fxyd1*$^{-/-}$ mice, suggesting that the amount of transmitter per vesicle and postsynaptic receptor responsiveness is unaltered in the absence of FXYD1. The frequency of mEPSCs tended to be lower in *Fxyd1*$^{-/-}$ mice (23.5 ± 6.2, n = 8) than in WT animals (33.4 ± 5.1, n = 19), but this difference did not achieve statistical significance, suggesting that the absence of FXYD1 may not result in a decreased probability of neurotransmitter release in hypothalamic neurones.

Fxyd1-deficient female mice have delayed puberty

To determine if these electrophysiological deficits would result in alterations in the initiation of puberty, we compared the age at vaginal opening and the age of the first oestrous in *Fxyd1*$^{-/-}$ mice and WT animals. As shown in Fig. 7, both the age at vaginal opening (Fig. 7A) and the age at first oestrous (Fig. 7B) were delayed in *Fxyd1*$^{-/-}$ mice ($p<0.02$ and <0.05, respectively). At 44 days of age, 50% of the WT animals had shown first oestrous, as compared to less than 20% of the KO mice. All WT mice had their first oestrous by 54 days of age, In contrast, at this time first oestrous was detected in only about 50% of the *Fxyd1*$^{-/-}$ mice. The age at first litter was also significantly ($p<0.05$) delayed in the mutant animals (Fig. 7C); however, the mating-delivery interval for the three subsequent litters was either similar in WT and mutant mice (litters 2 and 3) or slightly shorter ($p<0.05$) in the mutant animals (litter 4, Fig. 7D).

Discussion

The present results suggest that FXYD1 is a molecule involved in the homeostatic control of GnRH neurones, and that FXYD1 may exert this function by facilitating the response of these cells to transsynaptic excitatory inputs. Because FXYD1 is overexpressed in the brain of subjects affected by RTT and in a mouse model of this syndrome (14), it is possible that the earlier initiation of puberty we observed in girls suffering from RTT may be, at least in part, related to this facilitatory effect of FXYD1. It is also possible, however, that the advancement of puberty in RTT girls reflects an increased function of genes that, according to a recent study (41), are transcriptionally activated and not repressed by MECP2 in the hypothalamus of *Mecp2*-null mice. These animals reproduce most of the neuropathology of RTT (19-21). Nevertheless, it is formally possible that the transcriptional alterations seen in the hypothalamus of mice (which does not contain GnRH neurones) may not be identical to those that may occur in the hypothalamus of humans (which contains the bulk of the total population of GnRH neurones). Future research is required to distinguish between these possibilities.

That FXYD1 may contribute to the maturation of the excitatory transsynaptic control of GnRH secretion is suggested by the pattern of *Fxyd1* mRNA expression seen in the hypothalamus of pre- and peripubertal female rats. *Fxyd1* mRNA abundance first increases

at the beginning of the fourth week of postnatal life, a time of development when the open-loop, slow-frequency mode of gonadotrophin secretion subsides, and a faster, mature pattern of gonadotrophin output becomes established (reviewed in (38)). *Fxyd1* expression increases again after the first ovulation, suggesting that hypothalamic cells expressing this gene acquire mature levels of FXYD1 at the time when reproductive competence is attained. These changes in *Fxyd1* expression may play a role in the developmental control of GnRH neuronal function, because in the absence of FXYD1 the intrinsic excitability of GnRH neurones is significantly reduced, and both the initiation of puberty and the attainment of reproductive capacity are delayed. Whether this regulatory effect also involves a FXYD1-dependent modulation of clock mechanisms controlling GnRH output is an intriguing possibility that deserves future study.

Although our study does not address the issue of the potential role that FXYD1 may play in the homeostatic control of neuronal networks controlling GnRH neurones, it would not be unreasonable to assume that neuronal subsets expressing the *Fxyd1* gene may also be subjected to its regulatory influence. It is well established that GnRH secretion is regulated by both glutamatergic and GABAergic synaptic inputs (5-7,9,42,43), in addition to excitatory inputs provided by neurones that utilise kisspeptin as a neurotransmitter/neuromodulator (44). In turn, hypothalamic GABAergic neurones are innervated by glutamatergic neurones (10), so that their activity is subjected to glutamatergic regulatory control. Adding complexity to this elaborated neuronal control system, it is now clear that activation of $GABA_A$ receptors expressed on GnRH neurones excites, instead of inhibiting GnRH neuronal activity (1,2). Thus, GABA appears to be inhibitory only to neuronal subsets that are coupled to GnRH neurones via excitatory synapses (38,45), but its direct, $GABA_A$ receptor-mediated effects on GnRH neurones remain excitatory throughout postnatal life (1,2,46).

To estimate the degree to which FXYD1 affects the pre-synaptic excitatory input to GnRH neurones we determined the amplitude and frequency of spontaneous miniature excitatory postsynaptic currents (mEPSCs) under conditions that prevent both action potential firing (TTX block) and inhibitory activity (picrotoxin block).The results showed that the amplitude of mEPSCs was similar in GnRH neurones from WT and *Fxyd1*$^{-/-}$ mice, suggesting that the amount of excitatory neurotransmitter per synaptic vesicle and the response of postsynaptic receptors located on GnRH neurones are normal in the absence of FXYD1. There was, however, a tendency for the frequency of mEPSCs to be lower in GnRH neurones from *Fxyd1* null mice, suggesting that the absence of FXYD1 may be associated with a decrease in release probability, and consequently, a reduction in excitatory inputs to the GnRH neuronal network. The variability in frequency rate observed is not unexpected, if one assumes that only a fraction of neurones synaptically connected to the GnRH neuronal network may express the *Fxyd1* gene. Further work is necessary to determine if the excitatory input to GnRH neurones is, in fact, diminished in the absence of *Fxyd1*, as our results appear to imply.

Consistent with earlier observations examining other genes (1,47,48), we found that not all (~50%) GnRH neurones express the *Fxyd1* gene. This heterogeneity suggests that the GnRH neuronal network as a whole is endowed with a high degree of plasticity and redundancy that allow alternative subpopulations of GnRH neurones to compensate for losses in function affecting individual components of the network. In the present study, the physiological consequences of this arrangement were readily apparent, because *Fxyd1*-null mice had delayed puberty and delayed acquisition of reproductive capacity, but a seemingly normal adult reproductive capacity, as assessed by their ability to become pregnant and carry those pregnancies to term. Whether *Fxyd1*$^{-/-}$ mice have a normal reproductive span remains to be determined. It is interesting that girls affected by RTT also show a transient

change in the timing of puberty initiation. Although they had an earlier initiation of breast development (Tanner stage 2), the time of completion of the pubertal process (first menstruation) was similar to that described for non-affected girls (37). These findings suggest that, as in the case of delayed puberty caused by loss of *Fxyd1* expression in mice, the earlier initiation of puberty in RTT is followed by homeostatic compensation that results in reestablishment of normal neuroendocrine reproductive function.

Of interest is the observation that *Fxyd1* expression in the hypothalamus is much lower than that of *Fxyd7*, and yet, only a minority of GnRH neurones expresses *Fxyd7*. It was previously shown that although both proteins act as regulators of the Na+, K+ ATPase enzyme (23), only *Fxyd7* is specifically expressed in brain (26). This tissue distribution suggests that FXYD7 may play a predominant role in modulating Na+, K+ ATPase activity in regions where the *Fxyd7* gene is highly expressed (for instance, the cerebral cortex and the ventromedial nucleus of the hypothalamus), whereas FXYD1 may be more important in selected neuronal populations throughout the brain, including specific neuronal subsets of both the cerebral cortex (14) and the cerebellum (40), in addition to GnRH neurones (this study). A previous report showed that *Fxyd1* expression is elevated in the frontal cortex of subjects affected by Rett syndrome, and mice lacking *Mecp2* (14). Na+, K+ ATPase activity was reduced in *Mecp2*-null neurones of the frontal cortex, suggesting that when FXYD1 is in excess, the activity of the enzyme is reduced. Earlier studies using cardiac myocytes (23,24), and cerebellar tissue (40) had thoroughly documented this function.

Based on these considerations, it may be suggested that a mechanism underlying the reduction in GnRH neurone intrinsic excitability seen in *Fxyd1* KOs involves a more active Na+, K+ ATPase pump. An enhanced activity of the pump would result in a more efficient restoration of the transmembrane Na+ and K+ gradients after neuronal excitation, effectively reducing neuronal excitability to subsequent excitatory inputs (25). As a consequence of these changes, GnRH neurones lacking *Fyxd1* might be expected to exhibit a more negative membrane resting potential than WT neurones. This, however, was not the case, a result that is consistent with previous studies showing that small alterations in the pump's activity (such as those that occur under physiological conditions) result in only minimal alterations of the resting potential (49). It is currently believed that small changes in Na+, K+ ATPase activity mostly affects cytosolic Na+ distribution, which in turn leads to secondary redistribution of Ca^{2+} mediated by a $Na+/Ca^{2+}$ exchanger (NCX1). An increased NCX1 activity decreases cytosolic Ca^{2+} concentrations by transporting Ca^{2+} from the cytosol into sarcolemmal vesicles (50). FXYD1 has been shown to inhibit NCX1 activity (51,52), suggesting that in the absence of this regulation, NCX1 activity increases, reducing more effectively the transient increase in cytosolic Ca^{2+} concentration caused by neuronal excitation. The overall validity of this concept is supported by the findings that intrinsic neuronal excitability depends on the activation of a Ca^{+}-dependent transient (53), and that Na+ K+ ATPase pump inhibitors increase neuronal excitability by enhancing a Ca^{2+}-dependent conductance (54). It then follows that the net outcome of both an increased activity of the Na+, K+ ATPase pump and NCX1 would be the reduced neuronal excitability we have observed in the present study.

Of importance in this context is the finding that fAHP is increased in GnRH neurones lacking *Fxyd1*. Because in brain neurones fAHP results from the activation of calcium-dependent potassium conductances (55), the fAHP may increase in GnRH neurones of $Fxyd1^{-/-}$ mice due to an increase in the underlying calcium-dependent potassium conductance. Consistent with this view, the input resistance, which is the reciprocal of conductance, was significantly decreased in *Fyxd1*-deficient GnRH neurones. Adding credence to this interpretation is the fact that the increased fAHP we observed in hypo-excitable GnRH neurones lacking$Fxyd1^{-/-}$ mirrors the pattern of decreased fAHP found in

hyperexcitable neurones (56). However, the channels responsible for producing fAHP in GnRH neurones remain to be identified. Additional mechanisms may need to be postulated to explain the finding that GnRH neurones of the central mPOA are less active than GnRH neurones located in the dorso-lateral POA and yet, they exhibit an increase in both fAHP and input resistance.

When adults, male *Fxyd1*-null mice have been shown to display cardiac hypertrophy and reduced cardiac Na^+, K^+-ATPase activity (28), instead of the increased activity predicted by earlier mechanistic studies in which FXYD1 levels were manipulated in cellular expression systems (23,24). Although we did not measure Na+, K+ ATPase activity, our results are in line with the notion derived from these earlier studies, i.e., that FXYD1 is an inhibitory regulator of Na+, K+ ATPase pump. It is possible that the loss of enzyme activity seen in the heart of adult *Fxyd1* KOs may be due to the activation of compensatory mechanisms, or, as suggested by the authors of that study (28), secondary to cardiac hypertrophy.

Taken altogether, our results suggest that FXYD1 is a molecule used by GnRH neurones to modulate the response of individual components of the GnRH network to excitatory inputs. They also suggest that increases in FXYD1 availability may augment neuronal excitability, whereas a reduction in this availability causes the opposite change. It appears likely that FXYD1 is just one of several molecules contributing to a general mechanism of homeostatic regulation that provides GnRH neurones with functional plasticity in their response to transsynaptic regulation

Acknowledgments

We thank Ms. Maria E. Costa for performing the *in situ* hybridisation and immunohistofluorescence studies. We are grateful to Dr. Amy Tucker (U. of Virginia, Charlottesville, VA) for providing us with the *Fxyd1* null mice, and to Dr. Martin Kelly (Oregon Health & Science University, Portland, OR) for his valuable comments on the electrophysiology studies reported in this paper. We also thank Dr. Suzanne Moenter (U. of Virginia, Charlottesville, VA) for providing the breeder pairs for the transgenic GFP-GnRH mice. This research was supported by National Institutes of Health (NIH) grants HD-25123, Eunice Kennedy Shriver NICHD/NIH through cooperative agreement HD18185 as part of the Specialised Cooperative Centres Programme in Reproduction and Infertility Research, RR00163 for the operation of the Oregon National Primate Research Centre (SRO) and NS43330 (OKR), and by a grant from The International Rett Syndrome Association (IRSA). We are grateful to Drs. D.G. Glaze, J.L. Neul and K.J. Motil (Baylor College of Medicine, Houston, TX), and S.A. Skinner (Greenwood Genetic Centre, Greenwood, SC) of the Rare Disease Clinical Research Centre Rett Syndrome Consortium for allowing us to use the data of pubertal development in females affected by RTT.

References

1. DeFazio RA, Heger S, Ojeda SR, Moenter SM. Activation of A-type γ-aminobutyric acid receptors excites gonadotropin-releasing hormone neurons. Mol Endocrinol. 2002; 16:2872–2891. [PubMed: 12456806]
2. Yin C, Ishii H, Tanaka N, Sakuma Y, Kato M. Activation of A-type gamma-amino butyric acid receptors excites gonadotrophin-releasing hormone neurones isolated from adult rats. J Neuroendocrinol. 2008; 20:566–575. [PubMed: 18363808]
3. Lagrange AH, Ronnekleiv OK, Kelly MJ. Estradiol-17β and μ-opioid peptides rapidly hyperpolarize GnRH neurons: A cellular mechanism of negative feedback? Endocrinology. 1995; 136:2341–2344. [PubMed: 7720682]
4. Ottem EN, Godwin JG, Petersen SL. Glutamatergic signaling through the *N*-methyl-D-aspartate receptor directly activates medial subpopulations of luteinizing hormone-releasing hormone (LHRH) neurons, but does not appear to mediate the effects of estradiol on LHRH gene expression. Endocrinology. 2002; 143:4837–4845. [PubMed: 12446611]
5. Eyigor O, Jennes L. Expression of glutamate receptor subunit mRNAs in gonadotropin-releasing hormone neurons during the sexual maturation of the female rat. Neuroendocrinology. 1997; 66:122–129. [PubMed: 9263209]

6. Goldsmith PC, Thind KK, Perera AD, Plant TM. Glutamate-immunoreactive neurons and their gonadotropin-releasing hormone-neuronal interactions in the monkey hypothalamus. Endocrinology. 1994; 134:858–868. [PubMed: 7905410]
7. Eyigor O, Jennes L. Identification of glutamate receptor subtype mRNAs in gonadotropin-releasing hormone neurons in rat brain. Endocrine. 1996; 4:133–139. [PubMed: 21153268]
8. Clarkson J, Herbison AE. Development of GABA and glutamate signaling at the GnRH neuron in relation to puberty. Mol Cell Endocrinol. 2006; 254-255:32–38. [PubMed: 16781054]
9. Ojeda, SR.; Terasawa, E. Neuroendocrine regulation of puberty. In: Pfaff, D.; Arnold, A.; Etgen, A.; Fahrbach, S.; Moss, R.; Rubin, R., editors. Hormones, Brain and Behavior. Vol. Vol 4. Elsevier; New York: 2002. p. 589-659.
10. Thind KK, Goldsmith PC. Glutamate and gabaergic neurointeractions in the monkey hypothalamus: A quantitative immunomorphological study. Neuroendocrinology. 1995; 61:471–485. [PubMed: 7617124]
11. Satake S, Saitow F, Yamada J, Konishi S. Synaptic activation of AMPA receptors inhibits GABA release from cerebellar interneurons. Nat Neurosci. 2000; 3:551–558. [PubMed: 10816310]
12. Min M-Y, Melyan Z, Kullmann DM. Synaptically released glutamate reduces γ-aminobutyric acid (GABA)ergic inhibition in the hippocampus via kainate receptors. Proc Natl Acad Sci USA. 1999; 96:9932–9937. [PubMed: 10449797]
13. Sweadner KJ, Rael E. The FXYD gene family of small ion transport regulators or channels: cDNA sequence, protein signature sequence, and expression. Genomics. 2000; 68:41–56. [PubMed: 10950925]
14. Deng V, Matagne V, Banine F, Frerking M, Ohliger P, Budden S, Pevsner J, Sherman LS, Ojeda S. FXYD1 is an MeCP2 target gene overexpressed in the brains of Rett syndrome patients and Mecp2-null mice. Hum Mol Genet. 2007; 16:640–650. [PubMed: 17309881]
15. Naidu S. Rett syndrome: A disorder affecting early brain growth. Ann Neurol. 1997; 42:3–10. [PubMed: 9225679]
16. Bienvenu T, Carrié A, de Roux N, Vinet M-C, Jonveaux P, Cuvert P, Villard L, Arzimanoglou A, Beldjord C, Fontes M, Tardieu M, Chelly J. *MECP2* mutations account for most cases of typical forms of Rett syndrome. Hum Mol Genet. 2000; 9:1377–1384. [PubMed: 10814719]
17. Amir RE, Van den Veyver IB, Wan M, Tran CQ, Francke U, Zoghbi HY. Rett syndrome is caused by mutations in X-linked *MECP2*, encoding methyl-CpG binding protein 2. Nat Genet. 1999; 23:185–188. [PubMed: 10508514]
18. Wan M, Lee SS, Zhang X, Houwink-Manville I, Song HR, Amir RE, Budden S, Naidu S, Pereira JL, Lo IF, Zoghbi HY, Schanen NC, Francke U. Rett syndrome and beyond: recurrent spontaneous and familial MECP2 mutations at CpG hotspots. Am J Hum Genet. 1999; 65:1520–1529. [PubMed: 10577905]
19. Chen RZ, Akbarian S, Tudor M, Jaenisch R. Deficiency of methyl-CpG binding protein-2 in CNS neurons results in a Rett-like phenotype in mice. Nat Genet. 2001; 327:331.
20. Guy J, Hendrich B, Holmes M, Martin JE, Bird A. A mouse *Mecp2*-null mutation causes neurological symptoms that mimic Rett syndrome. Nat Genet. 2001; 27:322–326. [PubMed: 11242117]
21. Kishi N, Macklis JD. MECP2 is progressively expressed in post-migratory neurons and is involved in neuronal maturation rather than cell fate decisions. Mol Cell Neurosci. 2004; 27:306–321. [PubMed: 15519245]
22. Crambert G, Geering K. FXYD proteins: new tissue-specific regulators of the ubiquitous Na,K-ATPase. Sci STKE 2003. Jan 21.2003 2003(166):RE1.
23. Crambert G, Füzesi M, Garty H, Karlish S, Geering K. Phospholemman (FXYD1) associates with Na,K-ATPase and regulates its transport properties. Proc Natl Acad Sci U S A. 2002; 99:11476–11481. [PubMed: 12169672]
24. Zhang XQ, Moorman JR, Ahlers BA, Carl LL, Lake DE, Song J, Mounsey JP, Tucker AL, Chan YM, Rothblum LI, Stahl RC, Carey DJ, Cheung JY. Phospholemman overexpression inhibits Na +-K+-ATPase in adult rat cardiac myocytes: relevance to decreased Na+ pump activity in postinfarction myocytes. J Appl Physiol. 2006; 100:212–220. [PubMed: 16195392]

25. Lees GJ. Inhibition of sodium-potassium-ATPase: a potentially ubiquitous mechanism contributing to central nervous system neuropathology. Brain Res Brain Res Rev. 1991; 16:283–300. [PubMed: 1665097]
26. Béguin P, Crambert G, Monnet-Tschudi F, Uldry M, Horisberger J-D, Garty H, Geering K. FXYD7 is a brain-specific regulator of Na,K-ATPase alpha1-beta isozymes. EMBO J. 2002; 21:3264–3273. [PubMed: 12093728]
27. Ojeda, SR.; Urbanski, HF. Puberty in the rat. In: Knobil, E.; Neill, JD., editors. The Physiology of Reproduction. 2nd Edition. Vol. Vol 2. Raven Press; New York: 1994. p. 363-409.
28. Jia LG, Donnet C, Bogaev RC, Blatt RJ, McKinney CE, Day KH, Berr SS, Jones LR, Moorman JR, Sweadner KJ, Tucker AL. Hypertrophy, increased ejection fraction, and reduced Na,K-ATPase activity in phospholemman-deficient mice. Am J Physiol Heart Circ Physiol. 2005; 288:H1982–H1988. [PubMed: 15563542]
29. Suter KJ, Song WJ, Sampson TL, Wuarin J-P, Saunders JT, Dudek FE, Moenter SM. Genetic targeting of green fluorescent protein to gonadotropin-releasing hormone neurons: Characterization of whole-cell electrophysiological properties and morphology. Endocrinology. 2000; 141:412–419. [PubMed: 10614664]
30. Romero C, Paredes A, Dissen GA, Ojeda SR. Nerve growth factor induces the expression of functional FSH receptors in newly formed follicles of the rat ovary. Endocrinology. 2002; 143:1485–1494. [PubMed: 11897707]
31. Shahab M, Mastronardi C, Seminara SB, Crowley WF, Ojeda SR, Plant TM. Increased hypothalamic GPR54 signaling: A potential mechanism for initiation of puberty in primates. Proc Natl Acad Sci U S A. 2005; 102:2129–2134. [PubMed: 15684075]
32. Ma YJ, Junier M-P, Costa ME, Ojeda SR. Transforming growth factor alpha (TGFα) gene expression in the hypothalamus is developmentally regulated and linked to sexual maturation. Neuron. 1992; 9:657–670. [PubMed: 1327011]
33. Berg-von der Emde K, Dees WL, Hiney JK, Hill DF, Dissen GA, Costa ME, Moholt-Siebert M, Ojeda SR. Neurotrophins and the neuroendocrine brain: Different neurotrophins sustain anatomically and functionally segregated subsets of hypothalamic dopaminergic neurons. J Neurosci. 1995; 15:4223–4237. [PubMed: 7790907]
34. Simmons DM, Arriza JL, Swanson LW. A complete protocol for *in situ* hybridization of messenger RNAs in brain and other tissues with radiolabeled single-stranded RNA probes. J Histotechnol. 1989; 12:169–181.
35. Ma YJ, Costa ME, Ojeda SR. Developmental expression of the genes encoding transforming growth factor alpha (TGFα) and its receptor in the hypothalamus of female rhesus macaques. Neuroendocrinology. 1994; 60:346–359. [PubMed: 7545971]
36. Rossi DJ, Oshima T, Attwell D. Glutamate release in severe brain ischaemia is mainly by reversed uptake. Nature. 2000; 403:316–321. [PubMed: 10659851]
37. Herman-Giddens ME, Slora EJ, Wasserman RC, Bourdony CJ, Bhapkar MV, Koch GG, Hasemeier CM. Secondary sexual characteristics and menses in young girls seen in office practice: A study from the pediatric research in office settings network. Pediatrics. 1997; 99:505–512. [PubMed: 9093289]
38. Ojeda, SR.; Skinner, MK. Puberty in the rat. In: Neill, JD., editor. The Physiology of Reproduction. 3rd Edition. Academic Press/Elsevier; San Diego: 2006. p. 2061-2126.
39. Bourguignon J-P, Gerard A, Fawe L, Alvarez-Gonzalez M-L, Franchimont P. Neuroendocrine control of the onset of puberty: Secretion of gonadotrophin-releasing hormone from rat hypothalamic explants. Acta Paediatr Scand [Suppl]. 1991; 372:19–25.
40. Feschenko MS, Donnet C, Wetzel RK, Asinovski NK, Jones LR, Sweadner KJ. Phospholemman, a single-span membrane protein, is an accessory protein of Na,K-ATPase in cerebellum and choroid plexus. J Neurosci. 2003; 23:2161–2169. [PubMed: 12657675]
41. Chahrour M, Jung SY, Shaw C, Zhou X, Wong ST, Qin J, Zoghbi HY. MeCP2, a key contributor to neurological disease, activates and represses transcription. Science. 2008; 320:1224–1229. [PubMed: 18511691]
42. Brann DW, Mahesh VB. Excitatory amino acids: Evidence for a role in the control of reproduction and anterior pituitary hormone secretion. Endocrine Rev. 1997; 18:678–700. [PubMed: 9331548]

43. Herbison AE. Multimodal influence of estrogen upon gonadotropin-releasing hormone neurons. Endocrine Rev. 1998; 19:302–330. [PubMed: 9626556]
44. Han SK, Gottsch ML, Lee KJ, Popa SM, Smith JT, Jakawich SK, Clifton DK, Steiner RA, Herbison AE. Activation of gonadotropin-releasing hormone neurons by kisspeptin as a neuroendocrine switch for the onset of puberty. J Neurosci. 2005; 25:11349–11356. [PubMed: 16339030]
45. Terasawa E, Fernandez DL. Neurobiological mechanisms of the onset of puberty in primates. Endocr Rev. 2001; 22:111–151. [PubMed: 11159818]
46. Moenter SM, DeFazio RA. Endogenous gamma-aminobutyric acid can excite gonadotropin-releasing hormone neurons. Endocrinology. 2005; 146:5374–5379. [PubMed: 16123153]
47. Jasoni CL, Todman MG, Han SK, Herbison AE. Expression of mRNAs encoding receptors that mediate stress signals in gonadotropin-releasing hormone neurons of the mouse. Neuroendocrinology. 2005; 82:320–328. [PubMed: 16721036]
48. Parent AS, Mungenast AE, Lomniczi A, Sandau US, Peles E, Bosch MA, Ronnekleiv OK, Ojeda SR. A contactin-receptor-like protein tyrosine phosphatase beta complex mediates adhesive communication between astroglial cells and gonadotrophin-releasing hormone neurones. J Neuroendocrinol. 2007; 19:847–859. [PubMed: 17927663]
49. Blaustein MP. Physiological effects of endogenous ouabain: Control of intracellular Ca^{2+} stores and cell responsiveness. Am J Physiol. 1993; 264:C1367–C1387. [PubMed: 8392793]
50. Blaustein MP, Lederer WJ. Sodium/calcium exchange: its physiological implications. Physiol Rev. 1999; 79:763–854. [PubMed: 10390518]
51. Zhang XQ, Qureshi A, Song J, Carl LL, Tian Q, Stahl RC, Carey DJ, Rothblum LI, Cheung JY. Phospholemman modulates Na+/Ca2+ exchange in adult rat cardiac myocytes. Am J Physiol Heart Circ Physiol. 2003; 284:H225–H233. [PubMed: 12388273]
52. Mirza MA, Zhang XQ, Ahlers BA, Qureshi A, Carl LL, Song J, Tucker AL, Mounsey JP, Moorman JR, Rothblum LI, Zhang TS, Cheung JY. Effects of phospholemman downregulation on contractility and [Ca(2+)]i transients in adult rat cardiac myocytes. Am J Physiol Heart Circ Physiol. 2004; 286:H1322–H1330. [PubMed: 14684371]
53. Aizenman CD, Linden DJ. Rapid, synaptically driven increases in the intrinsic excitability of cerebellar deep nuclear neurons. Nat Neurosci. 2000; 3:109–111. [PubMed: 10649564]
54. McCarren M, Alger BE. Sodium-potassium pump inhibitors increase neuronal excitability in the rat hippocampal slice: role of a Ca2+-dependent conductance. J Neurophysiol. 1987; 57:496–509. [PubMed: 2435860]
55. Smith MR, Nelson AB, du LS. Regulation of firing response gain by calcium-dependent mechanisms in vestibular nucleus neurons. J Neurophysiol. 2002; 87:2031–2042. [PubMed: 11929921]
56. Nelson AB, Krispel CM, Sekirnjak C, du LS. Long-lasting increases in intrinsic excitability triggered by inhibition. Neuron. 2003; 40:609–620. [PubMed: 14642283]

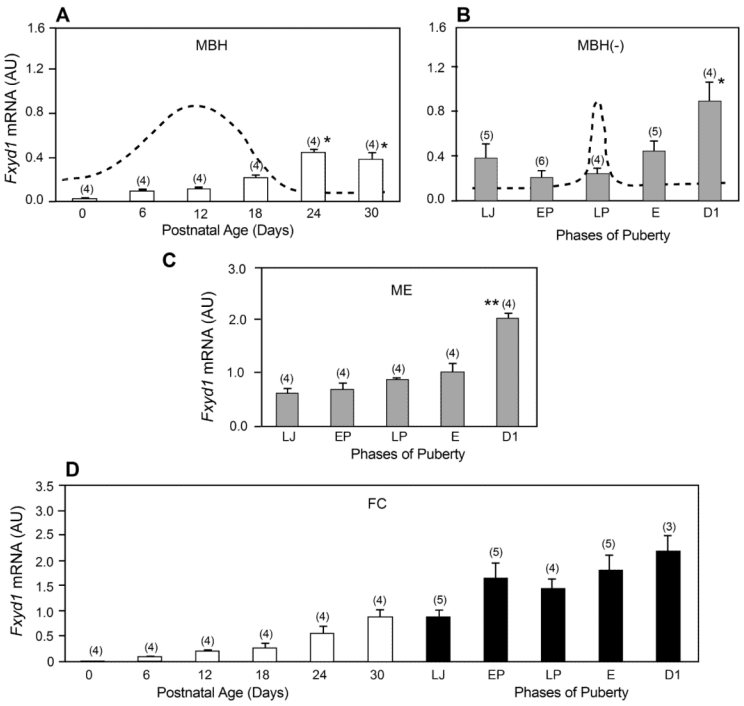

Figure 1.

Pre- and peripubertal changes in *Fxyd1* mRNA abundance in the medial basal hypothalamus (MBH), median eminence (ME) and frontal cortex (FC) of female rats, as assessed by real-time PCR. **A**, The MBH between PN day 0 (neonatal period) and 30 (late juvenile period), **B**, The MBH, without the ME (MBH-), at the time of puberty, **C**, The ME alone, **D**, The FC from PN day 0 to the end of the peripubertal phase, i.e. the day of first dioestrous. Bars are means and vertical lines are SEM. Numbers on top of bars are number of animals per group. LJ = late juvenile, similar to PN day 30; EP = early pro-oestrous; LP = late pro-oestrous, the day of the first preovulatory surge of gonadotrophins; E = first oestrous; D1 = first dioestrous. In A,*= $p<0.05$ vs. PN day 0 to 18; in B, * = $p<0.05$ vs. all other phases of puberty; in C,** = $p<0.01$ vs. all other phases of puberty. The stippled line in panel A represents the known profile of serum FSH levels during this phase of development (27). The stippled line in Panel B represents the known profile of serum LH levels observed at the time of puberty in female rats (27).

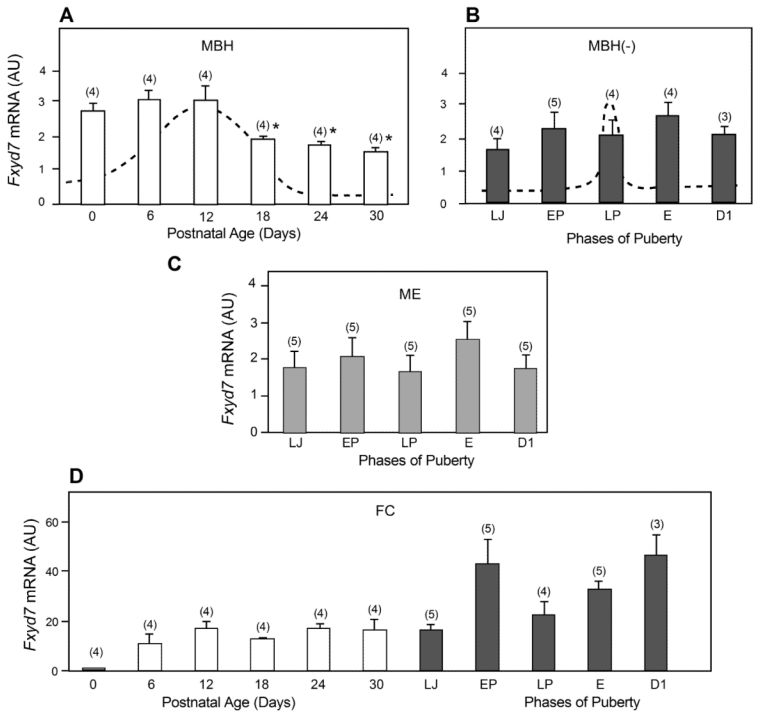

Figure 2.

Pre- and peripubertal changes in *Fxyd7* mRNA abundance in the medial basal hypothalamus (MBH), median eminence (ME) and frontal cortex (FC) of female rats, as assessed by real-time PCR. **A**, The MBH between PN day 0 (neonatal period) and 30 (late juvenile period), **B**, The MBH, without the ME (MBH-), at the time of puberty, **C**, The ME alone, **D**, The FC from PN day 0 to the end of the peripubertal phase, i.e. the day of first dioestrous. Bars are means and vertical lines are SEM. Numbers on top of bars are number of animals per group. For abbreviations see legend to Figure 1. In A,* = $p<0.05$ vs. PN day 12.

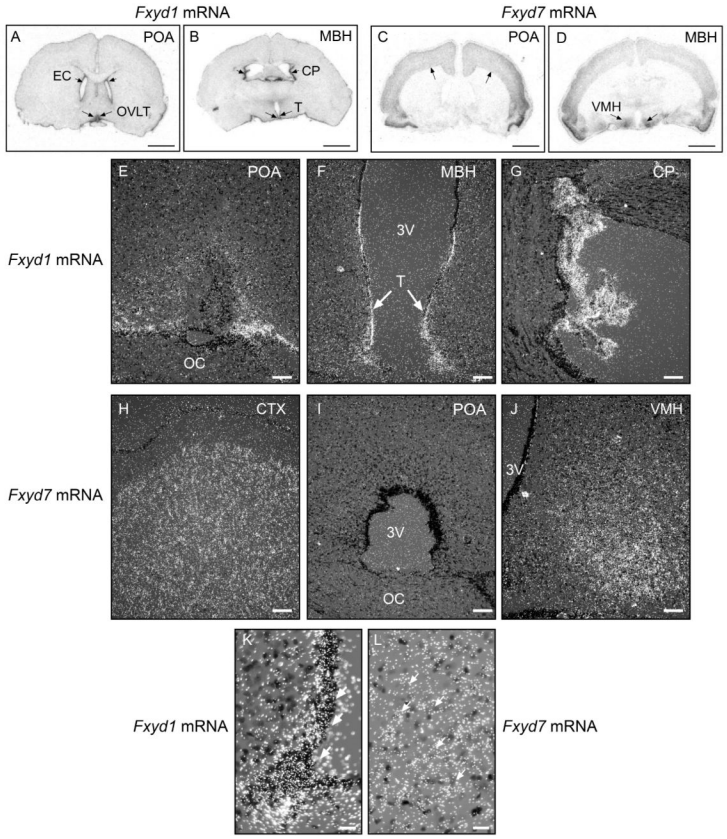

Figure 3.

Regional differences in *Fxyd1* and *Fxyd7* mRNA expression in the brain of prepubertal 28-day-old female rats as assessed by *in situ* hybridisation using ^{35}S-UTP labelled cRNA probes. **A**, Low magnification view of a coronal section of the rat brain at the level of the POA showing the distribution of *Fxyd1* mRNA transcripts. **B**, Similar view at the level of the MBH. **C**, Low magnification view of a coronal section of the rat brain at the level of the POA showing the distribution of *Fxyd7* mRNA transcripts. **D**, Similar view at the level of the MBH. Bars in A-D = 250 μm. **E**, Higher magnification view of the POA region showing the cellular sites of *Fxyd1* mRNA expression. **F**, The MBH, and **G**, The choroid plexus. **H**, Higher magnification view of the cerebral cortex showing the cellular sites of *Fxyd7* mRNA expression.. **I**, the POA, and **J**, The MBH. Bars in E-J = 100 μm. **K**, High magnification image of the ventrolateral aspect of the third ventricle showing that tanycytes express an abundance of Fxyd1 mRNA transcripts (examples denoted by white arrows). **L**, High magnification view of the VMH showing the presence of *Fxyd7* transcripts in cells with large, pale nuclei that, because of these characteristics, appear to be neurones (examples denoted by arrows). EC = ependymal cells; OVLT = organum vasculosum of the lamina terminalis; CP = choroid plexus; T = tanycytes; OC = optic chiasma; VMH = ventromedial nucleus; 3V = third ventricle.

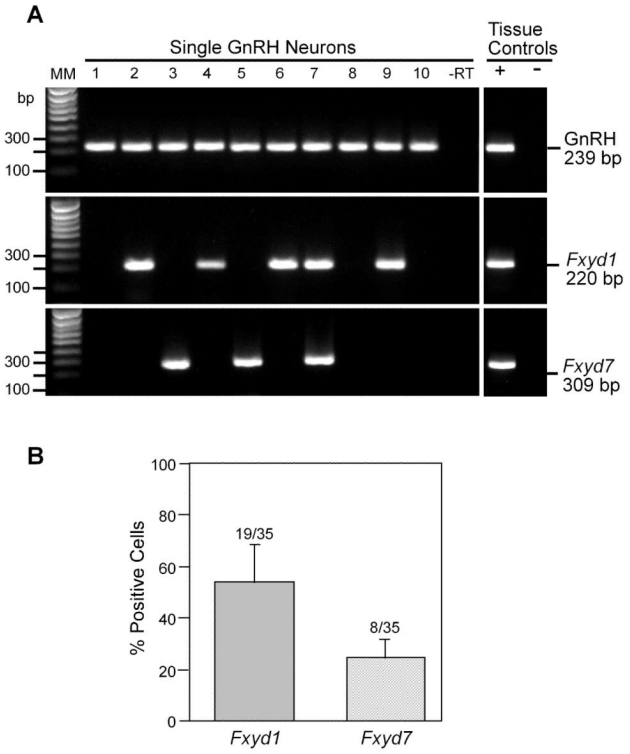

Figure 4.

Single cell RT-PCR identification of *Fxyd1* and *Fxyd7* transcripts in GnRH neurones from peripubertal (35-40-day-old) female mice. A representative gel illustrating that EGFP-GnRH neurones express the mRNAs encoding GnRH, FXYD1 and FXYD7 (also confirmed by sequencing). As a negative control, a cell reacted without reverse transcriptase (-RT) did not express any of the transcripts. POA positive (+, with RT) and negative (-, without RT) tissue controls were also included. Additional controls included artificial cerebrospinal fluid from the dispersed cellular milieu and water blanks, all of which were negative after RT-PCR (data not shown). MM, Molecular markers. Bar graph: Quantitative analysis of the expression of *Fxyd1* and *Fxyd7* mRNAs in GnRH neurones. Bars represent the mean ± SEM of the percent GnRH neurones expressing each of the *Fxyd* transcripts.

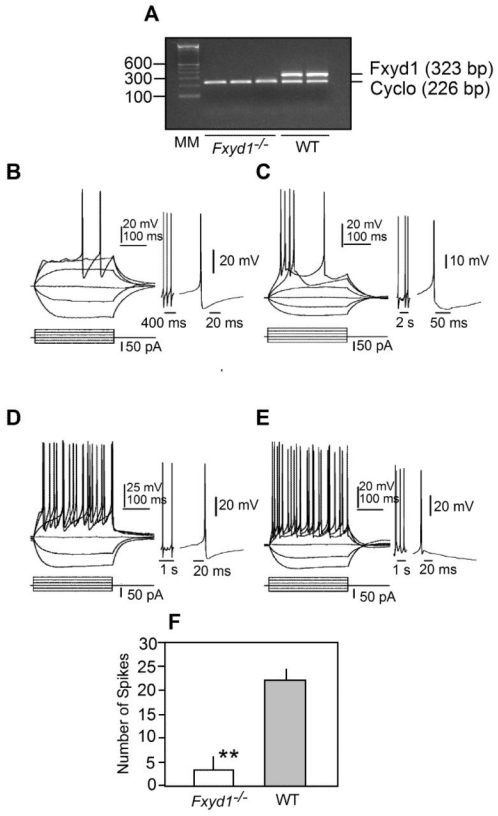

Figure 5.

Absence of *Fxyd1* mRNA in the MBH of *Fxyd1*$^{-/-}$ mice and responses of GnRH neurones from *Fxyd1*$^{-/-}$ and WT female mice to somatic current pulse injections. All recordings were done under current clamp conditions and using 28-30 day-old female mice. **A**, Gel image of a semi-quantitative PCR reaction demonstrating the absence of *Fxyd1* mRNA in the MBH of *Fxyd1*$^{-/-}$ female mice collected when the animals were 28 days of age. **B**, Response of a *Fxyd1*$^{-/-}$ GnRH neurone located in the central mPOA, **C**, Response of a *Fxyd1*$^{-/-}$ GnRH neurone located in the dorso-lateral mPOA, **D**, Response of a WT GnRH neurone in the central mPOA, **E**, Response of a WT dorso-lateral GnRH neurone. In each panel, the current pulse protocol is shown at the bottom and the responses at the top. Regardless of their *Fxyd1* genotype, GnRH neurones of the central mPOA always showed an fAHP response after an evoked action potential. This is illustrated as expanded tracings to the right of panels B-E. The expanded tracing to the right of panels B and C show the fAHP response of *Fxyd1*$^{-/-}$ neurones located centrally (B) or dorso-laterally (C) in the mPOA. The expanded tracing to the right of panel D shows a dorso-lateral WT GnRH neurone exhibiting fAHP, and the tracing to the right of panel E depicts a dorso-lateral GnRH neurones lacking fAHP. **F**, Quantification of the number of action potentials elicited by current pulse injection in GnRH neurones from *Fxyd1*$^{-/-}$ (n=10) and WT (n=12) animals. The resting membrane potential is -60 mV in B, C, and E; -58 mV in D. **, $p<0.01$.

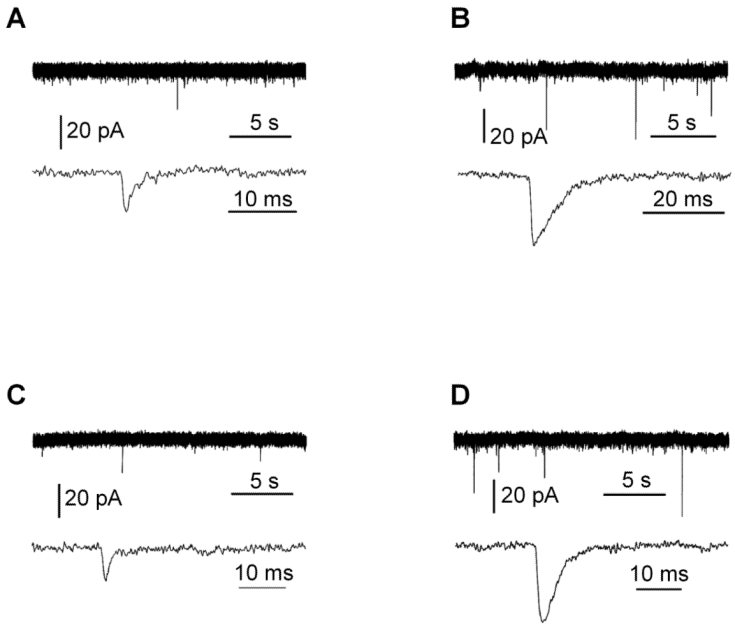

Figure 6.

Miniature excitatory postsynaptic currents (mEPSCs). All recordings were done under voltage clamp and in the presence of TTX (1 μM) and picrotoxin (100 μM) or bicuculline (35 μM), using 28-30 day-old female mice. In each panel, top traces shows miniature events over a longer period of time and low traces show expanded mEPSCs. **A**, **B**, mEPSCs in GnRH neurones from *Fxyd1*$^{-/-}$ mice. **C**, **D**, mEPSCs in WT GnRH neurones.

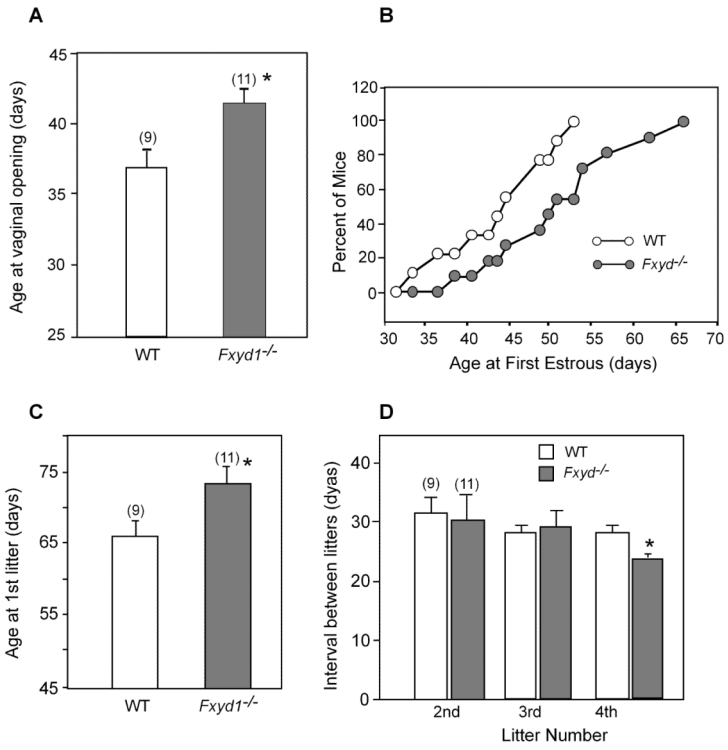

Figure 7.

Loss of *Fxyd1* expression delays female puberty in mice. **A**, Age at vaginal opening, **B**, Age at first oestrous, **C**, Age at delivery of first litter, **D**, Mating-delivery intervals for three consecutive litters delivered after the first litter. Bars are means and vertical lines are SEM. Numbers in parentheses on top of bars are number of animals per group. * = $p<0.05$, ** = $p<0.02$ vs. WT control.

Table 1

Input resistance and fast after- hyperpolarisation (fAHP) in GnRN neurones from WT and *Fxyd1*$^{-/-}$ mice

Groups	Input Resistance (GΩ)		fAHP (mV)	
	Central mPOA	Dorso-lateral mPOA	Central mPOA	Dorso-lateral mPOA
WT	1.67 ± 0.17 (10)	0.75 ± 0.08^{+} (9)	21.32 ± 1.60 (10)	13.71 ± 1.40^{+} (10)
Fxyd1-/-	1.32 ± 0.06*(11)	0.49 ± 0.02$^{*,+}$ (10)	29.84 ± 1.51* (9)	26.33 ± 1.92* (9)

Numbers in parentheses are number of cells per group

* = P<0.05 vs. WT control

$^{+}$ = P<0.05 vs.central mPOA